Available online at www.sciencedirect.com
ScienceDirect
Thermochimica Acta 470 (2008) 40–46
thermochimica acta
www.elsevier.com/locate/tca

TPR and XPS characterization of chromia–lanthana–zirconia catalyst prepared by impregnation and microwave plasma enhanced chemical vapour deposition methods

A. Dittmar *, D.L. Hoang, A. Martin

Leibniz-Institut für Katalyse e.V. an der Universität Rostock, Außenstelle Berlin, Richard-Willstätter-Str. 12, D-12489 Berlin, Germany

Received 23 November 2007; received in revised form 23 January 2008; accepted 27 January 2008
Available online 6 February 2008

Abstract

Chromia–lanthana–zirconia catalysts prepared by wet impregnation and microwave plasma enhanced chemical vapour deposition methods have been characterized by temperature-programmed reduction (TPR) and X-ray photoelectron spectroscopy (XPS). The impregnation procedure requires large amounts of solvent and calcination at high temperatures producing Cr^{6+} species. Unlike this, it is found that the microwave plasma enhanced chemical vapour deposition (PECVD) method predominantly produces Cr^{3+} species on zirconia-based supports. Moreover, it has been shown that the dispersion of chromium species deposited on zirconia-based support by the PECVD method is higher than the dispersion of those prepared by wet impregnation. Thus, the advantages of PECVD over the impregnation method consist in this case in preventing the use of large amounts of solvent and avoiding the primary formation of poisonous Cr^{6+} species as well as in enabling the deposition of chromium species with high dispersion on zirconia-based supports.

Keywords: Chromia-containing catalysts; Chromia–lanthana–zirconia; Temperature-programmed reduction; TPR; XPS; Impregnation; PECVD

1. Introduction

Chromium oxides supported on alumina, silica or titania have been known for many decades as highly active and selective catalysts for a wide range of important reactions, including polymerization, non-oxidative as well as oxidative dehydrogenation, hydrogenation, isomerization, aromatization and oxidation [1–3]. Recently, chromium oxides supported on pure or modified zirconia, because of the high thermal and chemical stability of the support, have been investigated as catalysts for aromatization [4], dehydrogenation [5–7] or combustion [8] of hydrocarbons as well. We have also found that chromium oxide supported on lanthana-doped zirconia, $CrO_x/La_2O_3–ZrO_2$, is able to catalyse the dehydrocyclization of C_{6+}-alkanes with promising selectivities for alkyl aromatics [9].

The properties of chromia–lanthana–zirconia catalysts strongly depend on the chemical and surface states of chromium oxides on zirconia-based supports [3–14]. This, in turn, may be influenced by preparation methods. Usually, chromium oxide supported catalysts are prepared by wet impregnation of corresponding supports with chromium-containing solvents followed by high temperature (HT) treatment in air. This procedure, on the one hand, is environmentally detrimental because of the necessity of using large amounts of solvents and the production of poisonous Cr^{6+} compounds [15,16]. This may strongly complicate the production and the storing of large amounts of Cr-containing catalysts. On the other hand, high temperature calcination unavoidably leads to sintering and/or agglomeration of chromium oxides, which may be the cause of catalyst deactivation and, therefore, prevents successful applications of catalysts. On the contrary, the low temperature microwave plasma enhanced chemical vapour deposition (PECVD) offers a non-conventional method for preparing chromium oxides on zirconia-based supports that avoids the use of large amounts of solvents and, therefore, it is environmentally more friendly. Moreover, with avoiding

* Corresponding author. Tel.: +49 30 6392 4456.
E-mail address: andrea.dittmar@catalysis.de (A. Dittmar).

0040-6031/$ – see front matter © 2008 Elsevier B.V. All rights reserved.
doi:10.1016/j.tca.2008.01.019

thermal treatment at high temperature as well, the PECVD method may allow the deposition of chromium oxides as the catalytically active components in the form of highly dispersed, nano-structured and stable species on supports.

The application of the PECVD method for preparing chromium oxides on zirconia-based supports was first reported in Refs. [17,18]. Concerning the lanthana-containing zirconia (LZ) support prepared by calcination with the procedure applied in this work, cf. Section 2, it is worth mentioning that its textural, structural and surface properties have been characterized in detail in Ref. [18] by X-ray diffraction, Raman spectroscopy, FT-IR spectroscopy and thermoanalysis, TG/DTA-MS. It was found that the calcination of lanthana-doped zirconium hydroxide forms the meta stable tetragonal phase, *t*-ZrO_2, with the composition $La_{0.1}Zr_{0.9}O_{1.95}$, in which the La^{3+} cations partly occupy the lattice sites of Zr^{4+} cations. The results also evidenced that the oxygen plasma treatment with low or medium microwave power, short treatment duration and moderate oxygen partial pressure used in this work, cf. Section 2, does not significantly change the bulk as well as surface chemical properties of the support. In particular, it does not affect the hydroxyl groups required for anchoring Cr species. In this paper, temperature-programmed reduction (TPR) and X-ray photoelectron spectroscopy (XPS) characterizations are used to compare redox behaviour and surface dispersion of chromium oxides supported on lanthana–zirconia support prepared by wet impregnation and by PECVD methods.

2. Experimental

2.1. Catalyst preparation

At first, the supports were prepared by calcination of lanthana-doped zirconium hydroxide (7.0 wt.% La_2O_3) supplied by MEL Chemicals, serial number XZO681/01 at 873 K for 4 h. The calcination procedure was described in detail in Ref. [18]. It is worth mentioning that, with respect to this calcination treatment, the supports used in this work are different from those that have been used in Refs. [9–14], where the hydroxide precursors were not pre-calcined at high temperatures. The samples used in Refs. [9–14] will be denominated below as CLZ.

2.1.1. Impregnation

In the impregnation method, the lanthana–zirconia obtained after calcination were immersed under stirring into aqueous solutions containing appropriate amounts of chromium precursor, $(NH_4)_2CrO_4$ (Fluka). By addition of ammonia aqueous solution, the solution was kept at pH of 10. While stirring, the water excess was slowly evaporated at 323–333 K. The products obtained were dried in a static air atmosphere at 393 K for 12 h and then calcined at 873 K for 4 h, resulting in lanthana–zirconia supported chromium oxides. The samples prepared by impregnation will be denominated below as (*x*)C/LZ-imp, where (*x*) indicates the chromium content, LZ the lanthana/zirconia and imp is the impregnation method.

2.1.2. PECVD

A Siemens microwave plasma chamber has been used for deposing chromium oxide on the zirconia and lanthana–zirconia supports. A mixture of the powdery catalyst support and chromium acetylacetonate, $Cr(acac)_3$, precursor (Merck, No. 802485) was placed into a quartz flask. This flask was mounted on a metallic rod that was placed into the recipient and rotated during the treatment by means of an electric rotary engine in order to achieve an even coating of the support. Thereafter the chamber was evacuated to 5 Pa before oxygen flow of 300 sccm (standard cubic centimeter per minute) was fed into the plasma chamber by a mass flow controller. The pressure of the chamber was controlled with a baratron. A 2.46 GHz magnetron together with a power supply was used for generating of microwaves and ignition of the plasma discharge. During the plasma treatment, $Cr(acac)_3$ is evaporated and adsorbed on the supports. The subsequent oxidative decomposition of adsorbed $Cr(acac)_3$, the mechanism has been discussed in detail elsewhere [17], forms supported chromium oxide species. The influences of microwave power, oxygen partial pressure and the PECVD treatment duration on the structural, textural and surface properties of catalysts were reported elsewhere [17,18]. In this work, for the purpose of comparison, the microwave power and oxygen partial pressure were kept constant for all samples prepared at 300 W and 70 Pa, respectively. The treatment duration depends on the carbonaceous amount of the samples, which resulted from the organic ligands of the chromium acetylacetonate, i.e. the plasma treatment was finished if no more carbon ($\leq$0.5 wt.%) was found by carbon–hydrogen analysis, separately performed by a CARLO ERBA combustion system. Below, the samples prepared by PEVCD will be denominated as (*x*)C/LZ-pl, where (*x*) indicates the chromium content, LZ the lanthana/zirconia and pl is the PECVD method.

2.2. Characterization

The apparatus for TPR experiments has been already described in detail in Ref. [14]. The experimental procedure consists of (i) the first reduction run (TPR1), (ii) the reoxidation and (iii) the second reduction run (TPR2). Such a procedure enables to examine the reduction–oxidation behaviours of supported Cr species. The TPR runs were carried out in 5.15% hydrogen in argon flow at a heating rate of 10 K/min. Optimum sample weights corresponding to a reduction gas flow rate of 15 ml/min had been estimated according to the equation by Monti and Baiker [19]. All the samples were treated in argon flow at 575 K for 1 h prior the TPR experiment, which was carried out from 323 to 1023 K. The reoxidation step was carried out in He flow containing 20% O_2 at 873 K for 1 h. With the samples (*x*)C/LZ-pl, TPR2 was followed by a second reoxidation at 873 K for 1 h, before the third reduction run (TPR3) was carried out with conditions of TPR1 and TPR2. The quantitative analysis of the TPR results was carried out by the method described elsewhere [12–14].

X-ray photoelectron spectra were recorded on a SAGE 100 spectrometer (SPECS) using a non-monochromatized Mg Kα source operating at 20 mA and 12.5 kV. The spec-

tra were referred to the Zr $3d_{5/2}$ peak of ZrO_2 at 182.2 eV for the ZrO_2 supported samples. For determining the binding energy and quantitative analysis, the peaks were fitted with Gaussian–Lorentzian curves after Shirley background subtraction. The obtained peak areas were divided by the element-specific Scofield factor and the analyser-specific transmission function to get the composition in the near-surface region. The assignment of XPS peaks was carried out based on the NIST X-ray Photoelectron Spectroscopy Database, Version 3.4 [20]. The intensity ratios of the Cr $2p_{3/2}$ and Zr $3d_{5/2}$ nominated peaks, I_{Cr}/I_{Zr}, were calculated and used for representing the relative near-surface concentrations of Cr [21].

BET surface area of the catalysts has been determined after calcination as well as after reduction by nitrogen adsorption at 77 K, using a surface analyser ASAP 2000M, Micromeritics and the content of chromium supported by the inductive coupled plasma-optical emission spectrometry (ICP-OES) method, using an Optima 3000 XL, PerkinElmer. The results are listed in Table 1. The apparent surface density (ASD) of chromium, representing the total number of Cr atoms per surface area units of calcined as well as reduced samples, are summarized in Table 1 as well. The ASD values have been calculated according to the formula proposed in Ref. [22]:

$$\mathrm{ASD\,(Cr\ atoms/nm^2)} = \frac{wN/(A \times 100)}{[(1 - wB)/(A \times 100)]S \times 10^{18}},$$

where w is the determined weight percent of the chromium supported, A the atomic weight, B the molar mass of CrOx, N Avogadro's number, and S is the BET surface area of the support. According to De Rossi et al. [23], the ASD of chromium represents the true Cr surface density only in the case of the samples with low Cr loading, i.e. Cr loadings below the surface saturation value. Nevertheless, because of its independence on the surface area, the ASD value may be considered as a useful parameter to express the Cr surface concentration of the catalyst samples investigated in this paper.

3. Results and discussion

3.1. TPR of C/LZ-imp

Fig. 1 shows TPR1 (a) and TPR2 (b) profiles of the LZ support and (*x*)C/LZ-imp ($x = 1.0$, 2.0 and 4.0) catalysts. Quantitative results of TPR1 and TPR2 on the LZ and C/LZ-imp, consisting of T_{max} values, amount of hydrogen consumed as well as changes of the Cr oxidation state ($n - m$), calculated therefrom after the equation [14]

$$\mathrm{Cr}^n + \left[\frac{n-m}{2}\right] \mathrm{H_2} \leftrightarrow \mathrm{Cr}^m + (n-m)\mathrm{H}^+,$$

are summarized in Table 2. For comparing purpose, the quantitative TPR results obtained with CLZ catalysts [14] are listed in Table 2 as well.

The TPR1 of the LZ support shows a wide hydrogen consumption peak of low intensity at $T_{max} \cong 850$ K. After reoxidation by air at 823 K for 1 h, cf. Section 2, the TPR2 of LZ exhibits almost the same hydrogen consumption peak, see

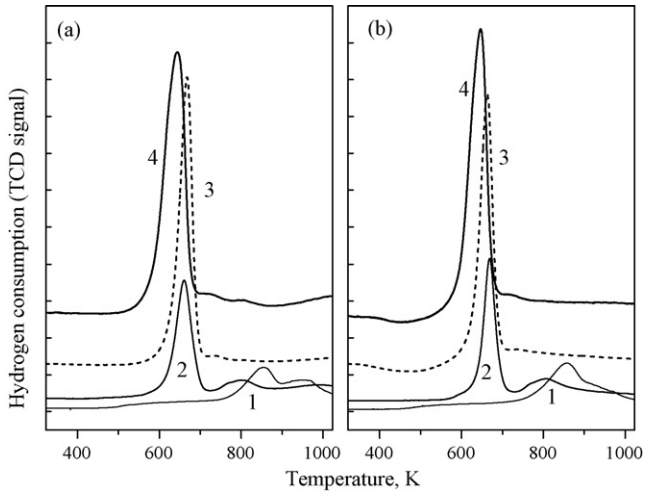

Fig. 1. TPR1 (a) and TPR2 (b) profiles of LZ support (1), (1.0)C/LZ-imp (2), (2.0)C/LZ-imp (3) and (4.0)C/LZ-imp (4).

Table 2, indicating the reversibility of hydrogen consumption on LZ during reduction–reoxidation treatments. This has been observed elsewhere on zirconia-based materials [14,24,25] and with high probability can be explained by the reversible transformation of a part of the Zr^{4+} and Zr^{3+} species on zirconia surfaces in oxidative and reductive atmospheres [26–28].

Like TPR of CLZ catalysts [14], the main hydrogen consumption signals are recorded in TPR1 at $T_{max1} = 642$–667 K with all the C/LZ-imp catalyst. This has been assigned elsewhere to the hydrogen consumed for reducing high valent Cr^{n+} ($n = 5$ or 6) species into Cr^{3+} [13,14]. As in case of CLZ catalysts, this T_{max1} value is slightly shifted to lower values with the increasing chromium loading, in detail from 667 to 642 K. The TPR2 profiles of C/LZ-imp, concerning the T_{max} position as well as the intensity of hydrogen consumption signals, cf. Table 2, do not significantly differ from the TPR1 ones. Although the hydrogen consumption peaks in TPR2 seem to be slightly narrower than the ones in TPR1 that may hint on the formation of a more uniform kind of Cr species after reoxidation, this similarity of TPR2 with TPR1 indicates a quantitatively reversibility of Cr species in C/LZ-imp samples in reduction–reoxidation treatments. This reversibility has been also observed in Refs. [12–14] and suggested to be caused by redox properties of La–Cr mixed oxide compounds, e.g. La_2CrO_6 and/or $LaCrO_4$. La–Cr compounds may be formed after catalyst calcination and, in consequence of esterification with surface hydroxyl groups, be anchored as real surface species on zirconia as overlayer. The shifting T_{max} to lower values with increasing Cr content, cf. Fig. 1 and Table 2, may be correlated with the decreasing strength of this anchoring. As evidenced by Raman spectroscopy [12,13], after being reduced during TPR1 to Cr^{3+}-containing species, these compounds on the catalyst samples containing $\leq$4 wt.% Cr can be restored again by reoxidation at 823 K.

Besides the main hydrogen consumption peak around 660 K, the TPR1 as well as TPR2 profile of (1)C/LZ-imp catalyst exhibits a wide hydrogen consumption peak of low intensity at higher temperatures with $T_{max} \cong 800$ K. At first glance, this seems to be caused by a partial reduction of the LZ support, see

Table 1
Cr content (wt.%), BET surface area (m^2/g) and Cr apparent surface density (Cr atoms/nm^2) of (*x*)Cr/LZ-imp and (*x*)Cr/LZ-pl samples

Catalysts	BET as-prepared (m^2/g)	ASD as-prepared (Cr atoms/nm^2)	BET after reduction (TPR2) (m^2/g)	ASD after reduction (TPR2) (Cr atoms/nm^2)
(1.0)C/LZ-imp	92	1.3	78	1.5
(2.0)C/LZ-imp	97	2.4	94	2.5
(4.0)C/LZ-imp	88	5.2	84	5.5
(0.6)C/LZ-pl	92	0.8	73	0.9
(0.7)C/LZ-pl	92	0.9	65	1.3
(0.8)C/LZ-pl	87	1.1	53	1.8
(1.3)C/LZ-pl	85	1.9	72	2.2
(1.4)C/LZ-pl	80	2.1	78	2.3
(1.5)C/LZ-pl	80	2.2	72	2.5
(1.7)C/LZ-pl	79	2.6	79	2.6
(2.0)C/LZ-pl	85	2.8	70	4.3
(4.2)CLZ-pl	120	4.4	103	5.1

above. As supposed in Ref. [14], the shifting of this high temperature TPR signal to lower temperature may perhaps be explained by an activation of hydrogen by chromium oxide species, facilitating the hydrogen uptake of LZ support. With increasing Cr content, however, unlike the CLZ catalyst, cf. [14], this second hydrogen consumption signal totally disappears as in the case of (2)C/LZ-imp, or appears only as shoulders as in the case of (4)C/LZ-imp sample. The reason for this different behaviour is not clear yet. It is supposedly related with the different ways of support treatment.

In Fig. 2, the amounts of hydrogen consumption (mmol/g_{cat}) measured during TPR1 and TPR2 are depicted versus the Cr loading of catalysts. For comparison, the hydrogen consumption theoretically expected for the total reduction of Cr^{5+} or Cr^{6+} to Cr^{3+}, which would required for an oxidation state change of $(n-m)=2$ or 3, respectively, are plotted in Fig. 2 as well. Apparently, Fig. 2 actually evidences the redox reversibility of Cr species supported on LZ by showing no significant differences between hydrogen amounts consumed during TPR1 and TPR2. With the samples containing $\leq$2 wt.% Cr, the amounts of hydrogen consumed during TPR1 and TPR2 correspond to the ones expected for the total reduction of Cr^{6+} or Cr^{5+} to Cr^{3+}. The

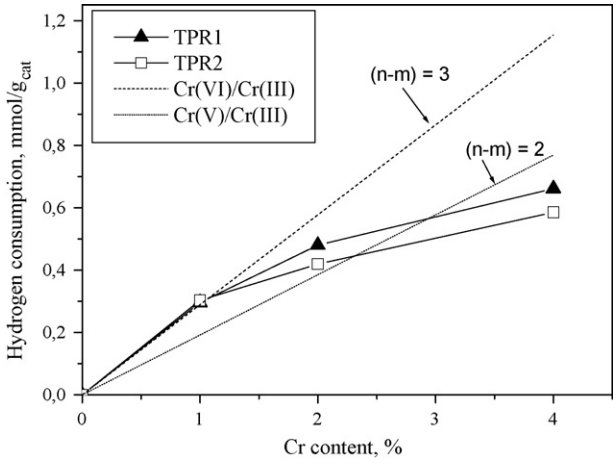

Fig. 2. Amounts of hydrogen (mmol/g_{cat}) consumed during TPR1 and TPR2 for reduction of Cr in (*x*)C/LZ-imp samples.

oxidation state changes listed in Table 2 are actually between 3.1 and 2.2. This indicates that the oxidation states of Cr, in calcined as well as reoxidized samples, should be +5 and/or +6, which is in line with the conclusions made elsewhere, e.g. in Refs. [3,6,12,13]. With the sample contains 4.0 wt.% Cr, the amount of hydrogen consumption strongly deviates from the expected one. This deviation is more pronounced than the one observed in Ref. [14] with CLZ catalysts, where the LZ support has not been pre-calcined at 873 K, cf. Table 2.

As described, the TPR1 and TPR2 behaviours of C/LZ catalysts are not basically different from the ones of CLZ and, therefore, can be similarly interpreted [14]. High valent species Cr^{6+}/Cr^{5+} are believed to be anchored by esterification with support hydroxyl groups up to saturation coverage. Beyond this saturation, i.e. beyond certain Cr content, which is determined by the nature of the support, excess Cr are converted to bulky and non-reoxidable Cr_2O_3 during calcination at high temperature [3,4,13]. Therefore, the more pronounced deviation observed on the C/LZ-imp samples, as shown in Fig. 2, can be caused by the transformation of excess and non-anchored Cr^{6+}/Cr^{5+} to Cr_2O_3 that can not more be reoxidized before TPR1 and TPR2. This also indicates that, in C/LZ-imp samples, Cr loading of ca. 2 wt.% reaches the support saturation coverage. The saturation coverage of the CLZ catalysts was shown to be higher, with Cr content of ca. 4 wt.% [14], which can correlated with higher amounts of hydroxyl groups required for esterification on non-precalcined support.

3.2. TPR of C/LZ-pl

Fig. 3 demonstrates TPR1 (a) and TPR2 (b) profiles of some (*x*)C/LZ-pl (*x* = 0.6, 1.4, 2.0 and 4.2) samples. Quantitative results of TPR1 and TPR2 are summarized in Table 2 as well, consisting of T_{max} values, amount of hydrogen consumed and changes of the Cr oxidation state $(n-m)$ calculated therefrom [14].

Like the calcined LZ, the PECVD treated LZ exhibits in TPR1 as well as in TPR2 almost the same hydrogen consumption peaks at ca. 850 K, cf. Fig. 1. This once more affirms that the plasma treatments applied in Section 2 does not affect the

Table 2
Quantitative TPR results: amounts of hydrogen consumed (mmol/g_{cat}), T_{max} and oxidation state change ($n-m$)[a]

Catalysts	Cr content (%)	TPR1				TPR2					Hydrogen consumption expected (mmol/g_{cat})	
		Hydrogen consumption, LT peak (mmol/g_{cat})	T_{max1} (K)	$n-m$	Hydrogen consumption, HT peak (mmol/g_{cat})	T_{max2} (K)	Hydrogen consumption, LT peak (mmol/g_{cat})	T_{max1} (K)	$n-m$	Hydrogen consumption, HT peak (mmol/g_{cat})	T_{max2} (K)	Cr(VI)/Cr(III)	Cr(V)/Cr(III)
LZ-cal	0.0				0.061	853				0.062	855		
C/LZ-imp	1.0	0.296	660	3.1	0.064	796	0.303	669	3.1	0.074	804	0.289	0.192
	2.0	0.480	669	2.5	–		0.419	663	2.2	–		0.577	0.385
	4.0	0.661	644	1.7	–		0.585	646	1.5	–		1.154	0.769
LZ-pl[b]					0.058	832				0.061	841		
C/LZ-pl	0.6	–		–	0.057	825/970	0.090	674	1.6	–		0.173	0.115
	1.4	–		–	0.065	762	0.313	654	2.3	–		0.404	0.269
	2.0	–		–	0.078	775/900	0.342	659	1.8	–		0.577	0.384
	4.2	–		–	0.125	775/970	0.581	635	1.4	–		1.212	0.808
CLZ[c]	1.0	0.287	688	2.9	0.062	815	0.235	693	2.4	0.064	810	0.289	0.192
	4.0	0.969	663	2.5	0.069	795	0.975	676	2.5	0.053	795	1.154	0.769

[a] Calculated from the intensity of the low temperature (LT) hydrogen consumption peak [14].
[b] Cr-free LZ support, calcined and treated in O_2-plasma.
[c] Already reported in Ref. [14].

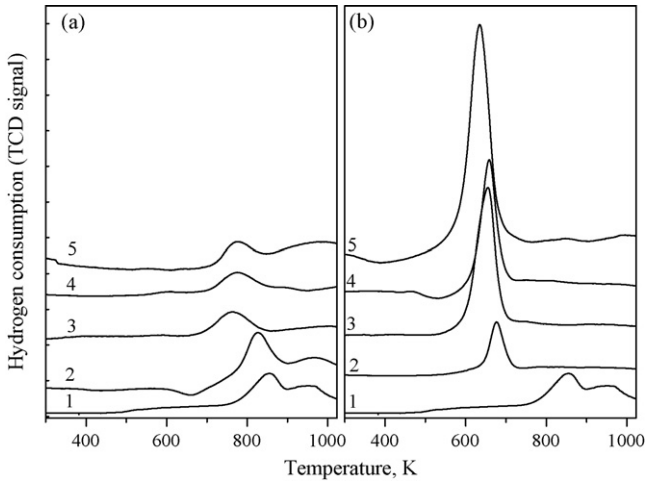

Fig. 3. TPR1 (a) and TPR2 (b) profiles of LZ pretreated by plasma (1), (0.6)C/LZ-pl (2), (1.4)C/LZ-pl (3), (2.0)C/LZ-pl (4) and (4.2)C/LZ-pl (5).

surface properties of LZ [18]. In Fig. 3a, the TPR1 profile of all the C/LZ-pl catalysts show weak hydrogen consumption signals at ca. 770–800 K and higher but no signals around 650 K being assigned to the reduction of Cr^{6+} and/or Cr^{5+} to Cr^{3+}. After reoxidation, cf. Section 2, however, these signals appear again in the TPR2, cf. Fig. 3b, as well as in the TPR3 profiles, which are not shown here. This restored signal is also shifted to lower temperatures with increasing Cr indicating, as supposed, different extend of anchoring. All this indicates that chromium ions deposited by PECVD on LZ support should be predominantly non-reducible, namely Cr^{3+}. XPS experiments confirm this suggestion by recording the Cr $2p_{3/2}$ peaks (not shown here) with the binding energy of around 576 eV characterizing chromium species of oxidation state (+3) as prevailing. With this finding, the advantage of the PECVD method over the impregnation was shown to consist in this case not only in preventing the use of solvents, as mentioned in Section 1, but also in avoiding the primary formation of poisonous Cr^{6+} species.

As described above, the TPR1 profiles of C/LZ-pl samples exhibit hydrogen consumption peaks at ca. 800 K. This may, as known, be caused by hydrogen consumption on the support. However, unlike Cr-free LZ (Figs. 1 and 3), C/LZ-imp (Fig. 1) and CLZ samples [14], this signal disappears in TPR2, even with low Cr loading. This complicates a clear and unequivocal assignment of these peaks. Furthermore, the restored TPR2 signals show T_{max} at the positions that are slightly different from the ones obtained for the C/LZ-imp or CLZ samples, cf. Table 2. The reasons for this result are not clear yet. It is supposedly related to different chemical forms of Cr species deposited by impregnation and by PECVD. For identifying such species, further investigations, e.g. by means of IR and/or Raman spectroscopy, will be required.

Fig. 4 depicts the amount of hydrogen consumed for reduction of Cr during TPR1, TPR2 and TPR3 in dependence on chromium loading. Apparently, hydrogen consumption is actually extremely low during TPR1, but it is drastically increased during TPR2 and the TPR3 hydrogen consumption does not differ from those of TPR2, quantitatively affirming

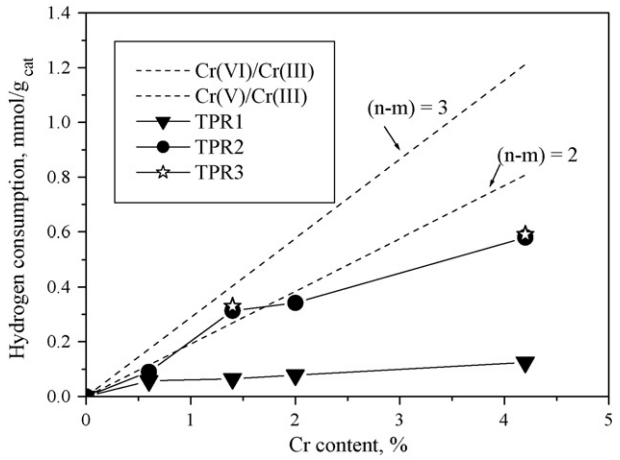

Fig. 4. Amount of hydrogen (mmol/g_{cat}) consumed during TPR1, TPR2 and TPR3 for reduction of Cr in (*x*)C/LZ-pl samples.

the reduction–reoxidation reversibility of Cr species deposited by PECVD on LZ support. Concerning this, they seem to be similar with the ones deposited by impregnation. However, it is worth noting that, unlike in the case of CLZ and C/LZ-imp catalysts, the hydrogen consumption amounts as well as $(n - m)$ values obtained in TPR2 and TPR3 for C/LZ-pl, particularly with the samples containing ≤2 wt.% Cr, cf. Table 2 and Fig. 4, rather correspond to the reduction of Cr^{5+} into Cr^{3+}. It may correlate with the differences of Cr precursors used in impregnation and PECVD deposition. At higher Cr content, the hydrogen consumption amounts also deviate from this, indicating, as discussed above, a formation of non-reoxidable Cr species, such as α-Cr_2O_3.

3.3. XPS of C/LZ-imp and C/LZ-pl

As described above, Cr species deposited on LZ support by impregnation as well as PECVD are more or less reversible in reduction–oxidation treatments. Such a reversibility of supported Cr, as argued in Ref. [14], should be correlated with their dispersed states, which can be estimated by the ratios of the Cr $2p_{3/2}$ and Zr $3d5_{/2}$ XPS peaks, I_{Cr}/I_{Zr} [20]. In Ref. [13], it has been shown that depicting the I_{Cr}/I_{Zr} ratios versus the Cr apparent surface density is useful for comparing the dispersion of Cr species on supports with different surface areas. Therefore, for comparing the dispersion of Cr species in C/LZ-pl with the one of chromium in C/LZ-imp, the I_{Cr}/I_{Zr} ratios obtained for as-prepared as well as reduced (after TPR2) samples are depicted in Fig. 5a and b, respectively, as function of chromium ASD, cf. Table 1.

Apparently, Fig. 5a shows that the I_{Cr}/I_{Zr} ratios of the as-prepared C/LZ-imp and C/LZ-pl samples increase linearly with increasing ASD between the values of 0.0 and 2.5–3.0 Cr atoms/nm^2, hinting on a uniform dispersion of Cr species within the limited saturation coverage that can be reached by Cr on zirconia-based supports [13,21,22]. With the ASD values ≥3.0 Cr atoms/nm^2, the I_{Cr}/I_{Zr} ratios of the catalysts prepared by impregnation decrease, indicating, in accordance with the TPR results, an agglomeration of non-anchored Cr into larger oxide cluster taking place during calcination. Unlike this, with the as-prepared C/LZ-pl catalysts, the I_{Cr}/I_{Zr} ratios are shown to increase almost linearly with increasing ASD between the values of 0.0 and 4.5 Cr atoms/nm^2, indicating a uniform dispersion of Cr species in a larger ASD range. After reoxidation followed by reduction (TPR2), cf. Fig. 5b, the I_{Cr}/I_{Zr} ratios of all the catalysts, prepared either by PECVD or by impregnation, decrease and show linearity only in a narrower range of ASD values between 0.0 and 2.5–3.0 Cr atoms/nm^2. This reveals the well-known impacts of oxidative and/or reductive treatments at high temperature causing additional agglomeration of Cr species [21,22]. However, with the same values of ASD, the I_{Cr}/I_{Zr} ratios obtained for the reduced C/LZ-pl samples remain still higher than the ones obtained for corresponding C/LZ-imp samples. It is worth mentioning that the $(n - m)$ values, cf. Table 2, obtained after TPR2 of the C/LZ-pl samples, except for the (1.4)C/LZ-pl, are almost independent of Cr loading. Moreover, although the hydrogen consumption for TPR2 is less than for the C/LZ-imp samples, the Cr dispersion is higher on the C/LZ-pl ones. The reason for this is not clear yet. It is not excluded that a portion of dispersed Cr^{3+} produced by PECVD is not more reoxidable. More detailed studies are required for clarifying this. It should be kept in mind that these Cr-containing catalysts have

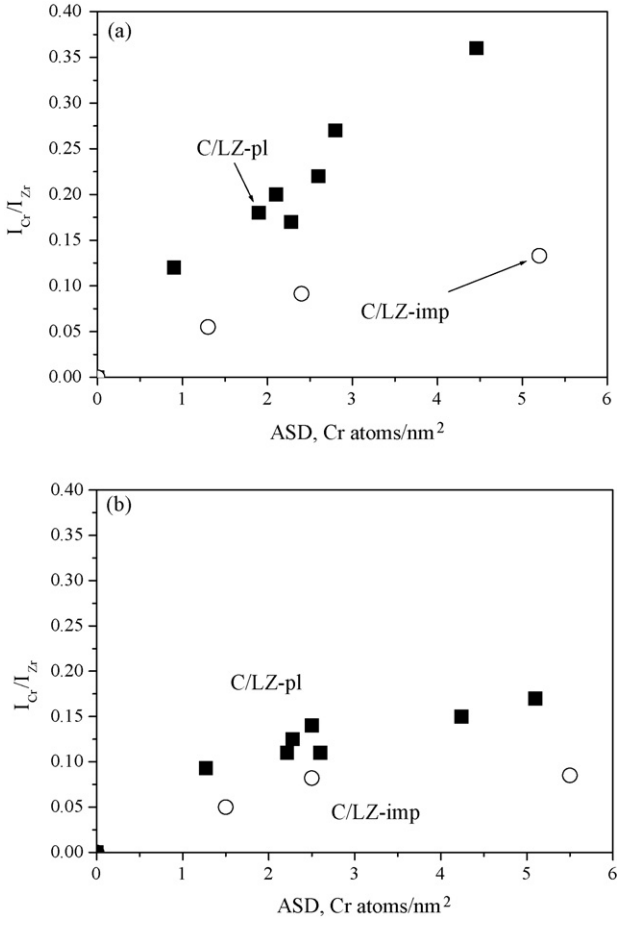

Fig. 5. The ratios of the Cr $2p_{3/2}$ and Zr $3d5_{/2}$ XPS peaks, I_{Cr}/I_{Zr}, for as-prepared (a) and reduced after TPR2 (b) as function of chromium ASD (Cr atoms/nm^2) on C/LZ-pl (■) and C/LZ-imp (◯) samples.

been prepared from different precursors, see Section 2, and this may influence the dispersion of Cr. Nevertheless, the comparisons made in Fig. 5 give clear hints that the PECVD method enables a deposition of Cr species on the LZ support with a higher dispersion than the wet impregnation. Since the dispersion of Cr species usually decisively influences the activity of Cr-containing catalysts, this may be an additional advantage of the PECVD preparation over the impregnation method.

4. Conclusions

The following conclusions can be drawn:

- It is found that, unlike the wet impregnation, the preparation of chromia–lanthana–zirconia catalysts by the plasma enhanced chemical vapour deposition method enables a deposition of Cr^{3+} species on zirconia-based supports. Therefore, it can be concluded that, besides preventing the use of large amounts of solvent, the advantages of the PECVD method over impregnation also consist in avoiding the primary formation of poisonous Cr^{6+} species.
- On lanthana-containing zirconia supports, the initial dispersion of Cr species deposited by the PECVD method is shown to be more higher than the one of Cr deposited by impregnation. The oxidative and/or reductive treatments at high temperature decrease the dispersion of Cr. However, within the certain Cr content, corresponding to ASD values of ca. 2.5 Cr atoms/nm^2, the Cr dispersion of the catalysts prepared by the PECVD method remains higher than the Cr dispersion of the catalysts prepared by wet impregnation.

Acknowledgements

Financial support by the Federal Ministry for Education and Research of the Federal Republic of Germany (project 03C3013), the EU (European Fund for Regional Development) and the Federal State of Berlin (Department for Science, Research and Culture) is gratefully acknowledged. The authors are responsible for the contents. The authors thank Mrs. G. Hidde, Mrs. K. Neitzel and Mrs. W. Ziesche for technical supports.

References

[1] Ch.P. Poole Jr., D.S. McIver, Adv. Catal. 17 (1967) 223.
[2] M.P. McDaniel, Adv. Catal. 33 (1985) 47.
[3] B.M. Weckhuysen, I.E. Wachs, R.A. Schoonheydt, Chem. Rev. 96 (1996) 3327.
[4] V. Indonina, Catal. Today 41 (1998) 95.
[5] T.V.M. Rao, G. Deo, J.-M. Jehhng, I.E. Wachs, Langmuir 20 (2004) 7150.
[6] M.G. Cutrufello, S. De Rossi, I. Ferino, R. Monaci, E. Rombi, V. Solinas, Thermochim. Acta 434 (2005) 62.
[7] S.T. Korhonen, S.M.K. Airaksinen, A.Q.I. Krause, Catal. Today 112 (2006) 37.
[8] (a) V.R. Choudhary, G.-M. Deshmukh, S.G. Pataskar, Catal. Commun. 5 (2004) 115;
(b) V.R. Choudhary, B.S. Uphade, S.G. Pataskar, Appl. Catal. A: Gen. 227 (2002) 29.
[9] H. Lieske, D.L. Hoang, US Patent 6,239,323 B1 (2001).
[10] A. Brückner, J. Radnik, D.L. Hoang, H. Lieske, Catal. Lett. 60 (1999) 183.
[11] A. Trunschke, D.L. Hoang, J. Radnik, H. Lieske, J. Catal. 191 (2000) 456.
[12] D.L. Hoang, A. Dittmar, M. Schneider, A. Trunschke, H. Lieske, K.-W. Brzezinka, K. Witke, Thermochim. Acta 400 (2003) 153.
[13] D.L. Hoang, A. Dittmar, J. Radnik, K.-W. Brzezinka, K. Witke, Appl. Catal. A: Gen. 239 (2003) 95.
[14] D.L. Hoang, H. Lieske, Thermochim. Acta 345 (2000) 93.
[15] A. Leonard, R.R. Lauwerys, Mutat. Res. 76 (1980) 227.
[16] J.P. Wise, S.S. Wise, S. Kraus, F. Shaffiey, M. Grau, T.L. Chen, Ch. Perkins, W.D. Thompson, T. Zheng, Y. Zhang, T. Romano, T. O'Hara, Mutat. Res. 650 (2008) 30.
[17] A. Dittmar, Thesis, June 2002, URL: http://edocs.tu-berlin.de/diss/2002/dittmar_andrea.pdf.
[18] A. Dittmar, H. Kosslick, D. Herein, Catal. Today 89 (2004) 169.
[19] D.A.M. Monti, A. Baiker, J. Catal. (1983) 323.
[20] NIST X-ray Photoelectron Spectroscopy Database (http://www.nist.gov).
[21] A. Cimino, G. Gazzoli, M. Valigi, J. Electr. Spectrosc. Relat. Phenom. 104 (1999) 1.
[22] A. Cimino, S. De Rossi, R. Dragone, G. Ferraris, D. Gazzoli, M. Valigi, J. Colloid Interf. Sci. 202 (1998) 278.
[23] S. De Rossi, M.P. Casaletto, G. Ferraris, A. Cimino, G. Mineli, Appl. Catal. A: Gen. 167 (1998) 257.
[24] C. DallĭAgno, A. Gervanisi, F. Morazzoni, F. Pina, G. Strukul, Z. Zanderighi, J. Catal. (1985) 96.
[25] D.L. Hoang, H. Lieske, Catal. Lett. 27 (1994) 33.
[26] S.S. Farrage, Thesis, Humboldt-Universität, Berlin, 2005.
[27] D. Eder, R. Kramer, Phys. Chem. Phys. 4 (2002) 795.
[28] Q. Zhao, X. Wang, T. Cai, Appl. Surf. Sci. 225 (2004) 7.